Original scientific paper

Design, Implementation and Experimental Testing of a Hybrid Power Supply of Remote Measuring Station in the Surveillance, Alert & Warning System (SAWS)

Željko V. Despotović, *Senior Member, IEEE,* and Marko Tajdić

Abstract — **The paper presents the design, implementation and experimental testing of a hybrid power supply of telecommunication and measuring equipment incorporated in remote measuring stations, which are an integral part of the global Surveillance, Alert & Warning System (SAWS) in the Republic of Serbia. In these systems, it is very important to provide autonomy of permanent, reliable and quality power supply. In this case, the power supply system is in effect based on the use of solar energy i.e., photovoltaic (PV), in combination with the mains power supply 230V, 50Hz. Solar power is the primary source of power during the day, while in night conditions the secondary power supply is a distribution power grid (more precisely, the distribution power which is used for supplying the night street lighting). This hybrid power system is realized with two controlled chargers (MPPT solar and mains with input power factor correction), battery bank 12V/110Ah with the corresponding system for its monitoring and secondary DC/DC power converters for supplying telecommunication and measuring electronic modules. The key implementation and experimental results obtained during the realization of a SAWS remote measuring station on the river Ub (municipality of Ub), will be presented in the paper.**

Keywords — **Hybrid power, power electronics, solar energy, MPPT charger, remote measuring, telecommunication.**

I. INTRODUCTION

THE hybrid power supply systems, as the name implies, combine two or more power sources for supplying of consumers. Generally speaking, hybrid power supply systems are usually using renewable energy sources (RES), such as solar and wind. This involves application of implementation of solar photovoltaic (PV) panels and wind

generators. Also, in some cases when greater power autonomy is required, diesel-electric generators (DEG) are used in the previous combination of RES [1]-[4].

Hybrid power supply systems are suitable for powering consumers at hard-to-reach (rural) locations, where there is no possibility of power supply from a distribution power grid or in cases when supplying from a power grid has a predominantly intermittent character [4]-[7].

Hybrid power supply systems are very efficient and reliable in the case of frequent mains power outages and mains power failure (so-called "black-out" intervals) [8]-[10].

These systems can usually store electricity, which is needed when consumption peaks occur or when the mains power is low. Storage is provided in rechargeable batteries, which increase the flexibility and reliability of the system. It is a very common case that the hybrid power supply of DC consumers at remote measuring stations (measuring electronics devices, telecommunication devices, etc.) is realized through a back-up power supply system [11]-[12].

In hybrid power supplies for crop irrigation systems, a DC/AC converter (inverter) is often used to power the pump set (single or three phase). In these systems, in addition to the battery bank, three sources are used: a DC source, typically solar panels, DC or AC wind generators and distribution AC power grid [13].

In previously described cases the AC power grid can compensate for the power supply interruption coming from solar panels or wind generators, and conversely the energy from solar panels and wind generators can cover any power grid failure that may occur. In the case that both power sources are not present, the role is taken over by the battery bank, which in that case provides autonomy [14]-[15].

This paper presents the design, realization and experimental testing of a specific hybrid power system, which is used for DC powering of telecommunication and measuring equipment of remote measuring stations, which are an integral part of the Surveillance, Alert and Warning System (SAWS).

The power supply is based on the use of solar energy (DC source) in combination with mains power supply (AC source). Solar power is the primary source of power during the day, while at night the distribution power grid is used as power (power from a street light pole).
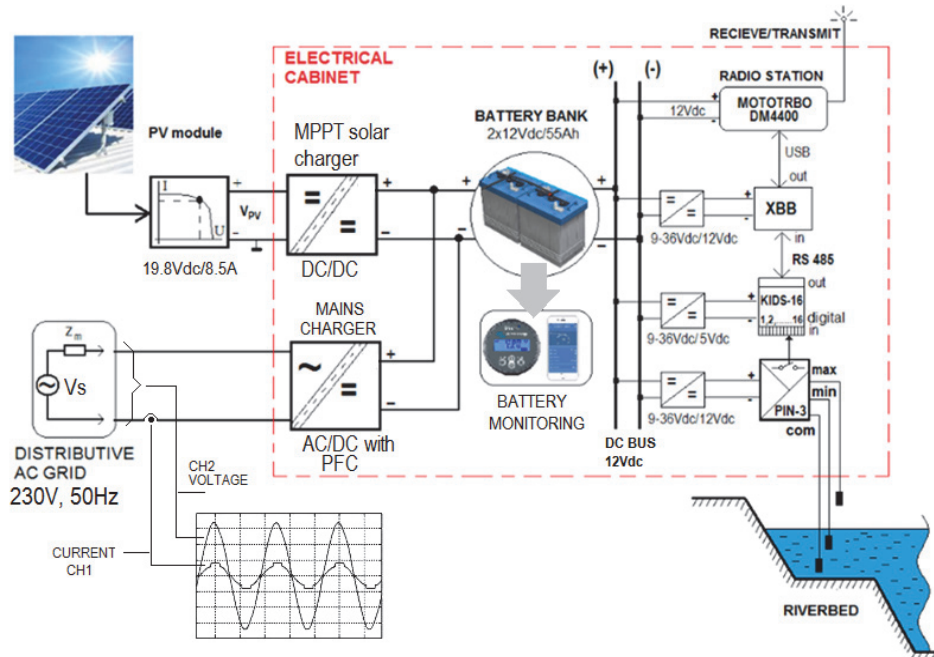
Fig. 1. Principal block diagram of powering remote measuring station.

The realized hybrid power supply system consists of several key units: (1) DC/DC solar charger with MPPT, (2) mains AC/DC charger with power factor correction (PFC), (3) battery bank 12V/110Ah including the corresponding monitoring system and (4) DC/DC power converters with secondary voltage stabilization for power of telecommunication and measuring electronics.

The paper is conceived as follows: a description of the realized hybrid power system is given in Chapter II, the remote station system consumers are described in Chapter III, Chapter IV represents the design of solar power, experimental results are given in Chapter V, the practical implementation of the hybrid power is shown in Chapter VI and finally conclusions are derived in Chapter VII.

II. DESCRIPTION OF REALIZED HYBRID POWER

The power supply block diagram of remote measuring station at a flood protection system on the river Ub is given in Fig. 1. The measuring and telecommunication system housed in an electrical cabinet is supplied from two power sources: a distributive AC grid and a solar panel. The grid power 230V, 50Hz is provided from the street lighting pole (the only accessible AC source that was set by a technical requirement by the investor-Emergency Management Sector of the Republic of Serbia (Command Control center Ub). The main disadvantage of this power source is that electricity is only provided during the night when street lights are in operation. The primary power source during the sunny part of the day is a solar panel. For previous reasons, in the power supply system are used two battery bank chargers. These chargers are mutually galvanically isolated. In each of chargers individually is provided isolation between the inputs and outputs terminals. One charger is solar, which is powered at the input via a solar panel with a maximum power of 168W (maximum voltage 19.4V and maximum current 8.5A), and the other is a mains charger,

which is powered from the input mains voltage 230, 50Hz.

The block diagram of an MPPT solar charger with associated protection and alarm functions is shown in Fig. 2.
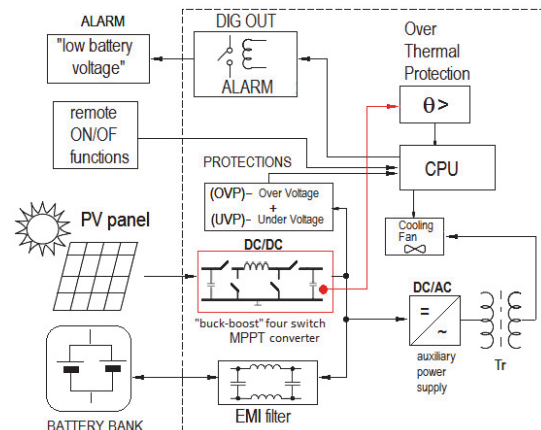

Fig. 2. The block scheme of MPPT solar charger with implemented protection and alarm functions.

The main and most important functional block of the solar charger is the MPPT controller which provides tracking the maximum power point of the solar panel. This circuit is actually a four MOSFET switches synchronous "buck-boost" DC/DC converter [16] that provides voltage and charging current stabilization for the battery bank in a wide range of input voltages from a PV panel. In order to eliminate electromagnetic interference, the battery bank is powered by an adequate EMI filter.

The main control unit is the CPU, within which the analogue input is performed: MPPT charger assembly temperature, digital inputs: over voltage protection (OVP) and under voltage protection (UVP), remote charger control ("remote ON / OF") and digital outputs: cooling fan control and relay output "low battery voltage".

The auxiliary power supply is actually a low power DC/AC converter, which provides a stable supply of a fan for cooling the solar MPPT charger via a galvanic isolated transformer Tr.

The block diagram of the AC grid charger is given in Fig. 3. The AC grid charger is, in fact, a complex converter system. It consists of: (1) an input mains rectifier (AC/ DC) i.e., mains pre-regulator with implemented input power factor correction (PFC) control, (2) a DC/AC H-bridge power converter with four MOSFET switches and with PWM control, (3) a step-down transformer Tr1 with a ferrite core for high frequency voltage conversion, (4) an output high frequency rectifier (AC/DC power converter) with an LC-filter for supplying the battery bank.
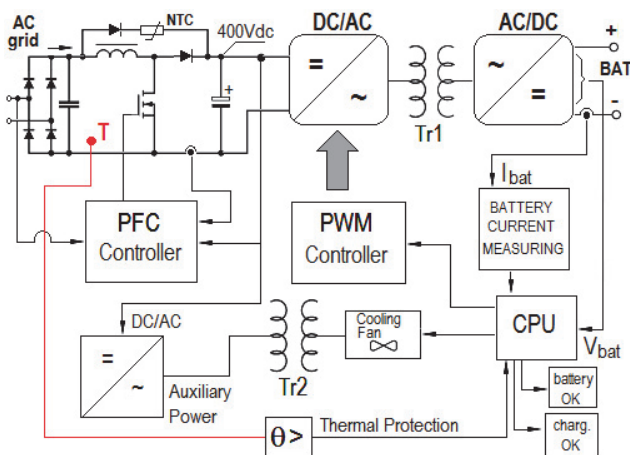

Fig. 3. AC grid charger block diagram with implemented protection and alarm functions and input power factor correction (PFC).

The input PFC pre-regulator with an associated PFC controller ensures that the power factor of the AC charger is greater than 0.95. Based on the measurement of input voltage, output current and output voltage of the PFC rectifier, the above function is provided. In this way, the level of harmonic distortion that this charger introduces into the AC power grid 230V, 50Hz is reduced to a minimum. A passive circuit, based on a resistor with negative temperature coefficient (NTC), is used to limit the starting input current of the PFC rectifier. The switching frequency of the PFC rectifier is 100 kHz. The output voltage of PFC rectifier (DC link voltage) is about 400Vdc and this is a supplying voltage for MOSFET H-bridge in DC/AC power converter. Also, from the 400Vdc power supply, a fan is supplied by means of a low-power DC/AC converter, which provides cooling of the complete charger.

The 400Vdc "H-bridge" power supply is galvanically isolated from the AC/ DC output rectifier, via a high-frequency step-up transformer Tr1, which is designed for a switching frequency of 50 kHz. The DC/AC H-bridge power converter and associated PWM controller provide the control of charging current and voltage of battery bank.

The PWM controller that controls the charging current and battery voltage is under the direct control of the central processor unit (CPU). The CPU sets the reference values, i.e., the time profile of the battery charging current and battery voltage as shown in time diagrams in Fig. 4.

The CPU monitors and controls the charging of the battery bank. For this purpose, two analog feedback loops were realized: one is the battery charging current feedback and the other the battery voltage feedback (as shown in Fig. 3).

The following signals are used as digital inputs to the CPU: an optically isolated remote control signal (so-called "remote-control" -RC), selection of charger mode (2-stage and 3-stage charge profile), detection of incorrect connection of battery ends (+ BAT) and (-BAT) and thermal protection (over temperature protection) if the PFC rectifier overheats.

The following statuses are derived from the CPU in the form of digital signals: connected battery ("bat OK") and correct charging mode ("charger OK"). Other digital outputs are: control the operation of the main switch that brings the battery bank to voltage (terminals +BAT, -BAT) and turn on the cooling fan if the temperature inside the charger module exceeds a predetermined value of the over temperature protection threshold.

The system has a 12Vdc/110Ah battery bank with a corresponding module for measuring battery voltage and current, as well as for the monitoring of characteristic battery states: voltage, current, capacity [Ah], degree of charge (so-called "state of charge" -SOC [%]), degree of discharge (so-called "state" of discharge "-SOD [%]), time to-go [h] and battery temperature [°C]. The battery bank is designed for deep discharge and has the possibility of cyclic charging and discharging.

The three-stage battery charging profile (voltage and current) from the mains charger is shown in Fig. 4.
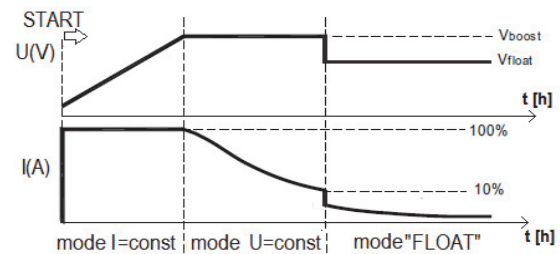

Fig. 4. Characteristic profiles of battery voltage and current using a mains charger.

In mode-I=const, a constant ten-hour charging current is provided (approximate value of about 10% of the capacity of the battery bank, i.e., I10h [A] ≈0.1·C [Ah]. In this mode, there is an approximately linear increase in battery voltage to the level Vboost. After reaching this level in the second so called U-mode, voltage regulation is provided, i.e., maintaining the constant battery voltage Vboost. In this mode, the battery current is falling to 10% of the initial charging current I10h [A]. After reaching this level, the charger switches to the "FLOAT" mode, and then the battery current is 0.1 • I10h [A] (in this mode there is a maintenance current called "trickle-charge"). Battery voltage is equal to Vfloat in this mode and it is less than the maximum value of Vboost.

III. CONSUMERS IN HYBRID POWER SYSTEM

Within the principal block diagram in Fig. 1, consumers are shown (electronic equipment of the measuring and telecommunication system) at the remote station on the river Ub. The basic units of this system are: (1) a digital radio station MOTOTRBO DM4400-Motorola, (2) an XBB data acquisition module, (3) a KIDS digital input module and (4) a level indicator (min/max). All the mentioned consumers in this system are powered by DC buses that are at a voltage of 12V.
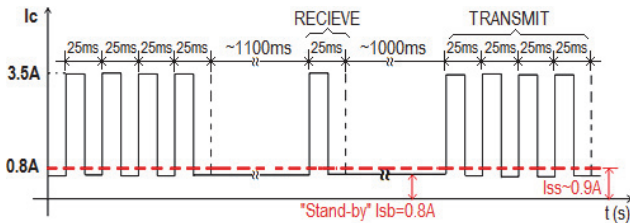

Fig. 5. Characteristic pulses of current consumption of digital radio station MOTOTRBO DSM 4400 Motorola.

The highest consumer of power in this system is the digital radio station. The task of the digital radio station is to send information about a water level and possible unwanted rise in the water level on the river Ub. As shown in Fig. 5, the current consumption of the radio station in this system, when it operates in TRANSMIT mode is max 3.5A for 100ms (4 pulses for 25ms, with a pulse / pause ratio of 50%), while in the RECEIVE mode the current consumption is max 3.5A (1 pulse duration 25ms). In standby mode, the consumption of a digital radio station is about 0.8A.

The Atlas XBB-RTL module (made in the Mihajlo Pupin Institute-Automation & Control System Ltd.) is a multifunctional process computer, data concentrator and protocol converter. It has the ability to process data in real time using PLC algorithms created according to the IEC 61131-3 standard. This device reliably collects data from measuring devices using different protocols. The collected and processed data can be presented locally (HMI) and/or sent to the monitoring on a SCADA server. The power supply of this module is realized directly from the DC/DC converter 9Vdc ÷ 36Vdc/12Vdc and the consumption of this module is about 2.5W.

The digital input module KIDS-16 (made in Mihajlo Pupin Institute-Automation & Control System Ltd.) has the ability to accept up to 16 digital inputs, which are then forwarded via the RS485 bus to the XBB process computer. The digital input module has an LED indication of active signals and serial communication. The power supply of this module is achieved by a DC / DC converter 9Vdc ÷ 36Vdc/5 Vdc. The consumption of this module at 5Vdc is about 100mA.

The three-electrode conductive indicator of the water level PIN-3 (product of the Mihajlo Pupin Institute) is a module that was applied to detect the water levels min/max in the riverbed. Additional power supply stabilization of this electronic circuit is achieved by a DC/ DC converter for the input voltage in a range of 9Vdc ÷ 36Vdc, while the output voltage is stabilized at 12Vdc. The maximum

consumption of this device at 12Vdc is around 500mA.

Considering the consumption of all devices under the most unfavorable exploitation conditions, it was adopted that data transfer by digital radio station is performed during 24 hours and that all consumers are active with the consumption currents that are given in Table 1.

TABLE 1: CURENTS AND POWER CONSUMPTION OF CONSYMERS IN THE SYSTEM.

Consumer (description)	Voltage (V)	Current (A) (AVG value)	Power (W)
PIN-3	12	0.10 (0.50)*	1.2 (6.0)
KIDS-16	12	0.05	0.6
XBB	12	0.25A	3.0
Radio Station	12	0.90A	10.8
TOTAL	-	**1.3 (1.7)**	**15.6(20.4)**

*current in steady state when the output relay switch is not activated (MAX level detection)

Based on this, we come to the total daily consumption of the measuring and telecommunication system expressed in [Ah], i.e. $C = 1.7A \cdot 24h = 40.8Ah$. Considering that all consumers are supplied with voltage $U = 12Vdc$, the daily electrical energy consumption for this system achieves the value of $E = C \cdot U = 40.8Ah \cdot 12V = 489.6Wh \approx 490Wh$.

IV. DESIGN OF SOLAR SYSTEM

The first step in designing the solar power supply of measuring station is to determine the exact position of the measuring point on the river Ub and to determine the optimal angle of inclination of the PV panel. In the PVGIS program, it was obtained that the latitude of a given place is 44.456°, and the longitude is 20.074°. For the given coordinates, the optimal values of the angle of inclination of the solar panel are obtained in the PVGIS program (the sun rays fall at a right angle to the surface of the panel) by months during the year, as given in Table 2. It is assumed that the solar panel is oriented to the south side (north-south direction).

TABLE 2: OPTIMAL MONTHLY SOLAR PANEL INCLINATION ANGLE BY MONTH AND DETERMINATION OF AVERAGE ANNUAL OPTIMUM

MONTH	OPT. ANGLE[°]
JANUARY	64
FEBRUARY	55
MARCH	44
APRIL	32
MAY	24
JUNE	21
JULY	24
AUGUST	32
SEPTEMBER	44
OCTOBER	56
NOVEMBER	64
DECEMBER	67
AVG ANNUAL OPTIMUM	**35**

Fig. 6 shows the average monthly values of irradiation [kWh/m²] in the longer annual interval (2005-2016) for a

given location and for the optimal values of inclination angles of 35° and 64°.

The inclination angle of 64° refers to the month with the lowest insolation (January). These diagrams show the extreme value of irradiation (lowest value), which was present at the beginning of 2011 (red dashed contour of Fig. 6). Irradiation values in the extreme case were taken into account in the calculation.
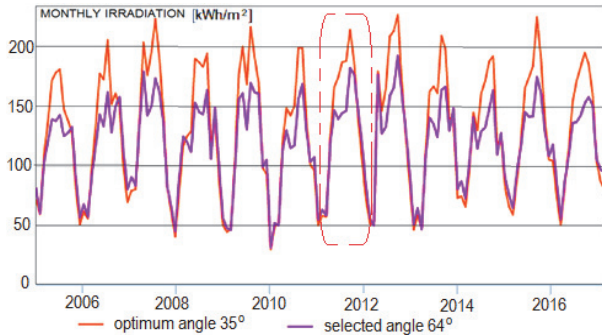

Fig. 6. Average annual irradiations (2005.-2016.) for the Ub location (according to PVGIS) for an optimal inclination angle of 35º and a selected angle of 64º.

Based on Table 3 (inclination angle of 35°), it is possible to calculate the total annual irradiation for 2011 year:
ΣH35=57.05+57.55+124.58+165.89+173.9+186.72+187.26+213.73+186.77+140.49+104.9+71.82=1671kWh/m²

The average value of daily solar irradiation for the most unfavourable month – January, in this case is H35_1 =57.05/31= 1840.32Wh/m².

TABLE 3: MONTHLY IRRADIATIONS - EXTREME CONDITIONS FOR 2011. YEAR) AND INCLINATION ANGLES 35 ° AND 64°.

MONTH	Monthly Irradiation for 2011 [kWh/m²]	
	incl. angle 35°	incl. angle 64°
JAN	57.05	63.32
FEB	57.55	58.42
MAR	124.58	119.24
APR	165.89	146.28
MAY	173.90	139.10
JUNE	186.72	144.08
JULY	187.26	145.75
AUG	213.73	181.58
SEP	186.77	176.73
OCT	140.49	146.98
NOV	104.90	118.45
DEC	71.82	82.90

Based on Table 3 (inclination angle of 64°), it is possible to calculate the total annual irradiation for 2011 year:
ΣH64=63.32+58.42+119.24+146.28+139.1+144.08+145.75+181.58+176.73+146.98+118.45+82.9=1523kWh/m²

The average value of daily solar irradiation for the month of January, in this case is H64_1=2042.58Wh/m².

Based on the previously calculated values, it is concluded that the total energy of solar radiation on the solar panel is about 10% higher at an inclination angle of 35°, but in the most unfavorable month of January, about 11% less energy would be obtained during the day.

It is possible to select one of two criteria for designing a solar power supply: (1) obtaining maximum energy from solar panels in the most unfavorable month of the year, or (2) maximum energy production from solar panels throughout the year.

If the first criterion is selected, the angle of inclination of the panel would be set to 64°, while in the case of the second criterion, that angle should be set to 35°. Considering that in addition to solar panels, another source-power grid 230V, 50Hz is also available, the second criterion was selected in the calculation. The "Peak Sun Hour" (PSH) time interval is calculated according to the relation:

$$PSH = \frac{H_{35\_1}[Wh/m^2]}{1000[W/m^2]},\qquad(1)$$

$$PSH = \frac{1840.32[Wh/m^2]}{1000[W/m^2]} \approx 1.84h.$$

Assuming that in addition to a solar panel, another source of electricity is available during the night (230V, 50Hz power grid), as well as the fact that the efficiency of MPPT controllers is about 90%, and battery efficiency 90% (obtained from the manufacturer's catalogue), the required power of solar panel under these conditions is:

$$P_{pv} = \frac{E/2}{PSH \cdot \eta_{reg} \cdot \eta_{bat}}.\qquad(2)$$

The calculation gives the value of the solar panel power:

$$P_{pv} = \frac{E/2}{PSH \cdot \eta_{reg} \cdot \eta_{bat}} = \frac{490Wh/2}{1.84h \cdot 0.9 \cdot 0.9} = 164W.$$

The LX160M –Luxor solar panel was adopted, with voltage /current data 19.74V/8.36A., at the point of maximum power. The required capacity of the battery bank is calculated from the relation:

$$C_{bat}[Ah] = \frac{E[Wh] \cdot N_d}{U_{bat}(V) \cdot \eta_{bat} \cdot \delta_{bat} \cdot K_t}\qquad(3)$$

where:

$E[Wh]$ -energy consumption

N_d -required number of days of system autonomy without both power sources (solar and mains power)

$U_{bat}[V]$ - rated battery voltage

$\delta_{bat}[\%]/100$ - allowable battery discharge of depth (DOD%)

$\eta_{bat}[\%]/100$ - battery efficiency

K_t - battery capacity correction factor due to ambient temperature (temperature range - 25°C…+40°C)

Taking into account the assumptions that the autonomy of the system is in the interval of 24h (i.e. Nd = 1), the battery efficiency of 90%, the discharge depth of 70% and the battery capacity reduction factor $K_t = 0.6$ due to unfavourable temperature condition, the obtained battery capacity is:

$$C_{bat}[Ah] = \frac{490[Wh] \cdot 1}{12(V) \cdot 0.9 \cdot 0.7 \cdot 0.6} = 108Ah.$$

A 12V/110Ah battery bank capacity was selected (two 12V/55Ah batteries, connected in parallel). The mains charger and MPPT charger are designed for output current of 16A, that they can simultaneously provide a battery bank

charging current of 14Amax and current of 2A for all consumers in the system.

V. EXPERIMENTAL TESTING OF HYBRID POWER

After the installation of the hybrid power supply, experimental testing and appropriate measurements were performed in order to verify the operational characteristics. The following measuring equipment was used to verify the hybrid power supply:

• Oscilloscope: Wave ACE 1002, 60MHz, 1Gs/s, TELEDYNE LECROY

• Current probe for oscilloscope: HANTEK CC650, range 0...±650A DC/AC

• Current probe with transducer for oscilloscope: AM503 Current Probe Amplifier Hewlett Packard

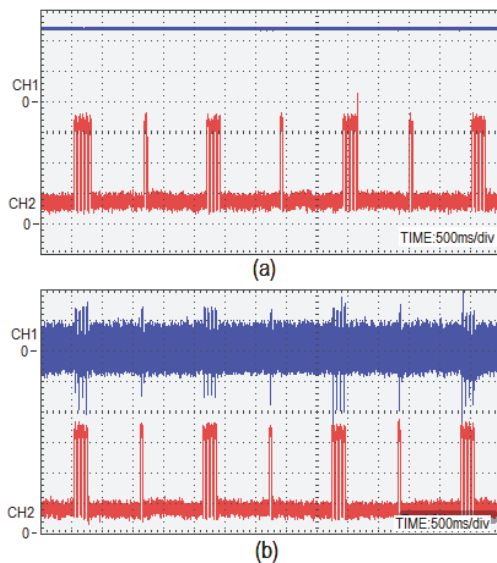• Hand current probe: AC, DC: UNI T- UT210E

• Multi-meter: PEAK TECH

Fig. 7. Measuring of radio station consumption; (a) consumption from 12Vdc: CH1-battery voltage [5V/div], CH2- current consumption of radio station [1A/div], (b) consumption from 230Vac: CH1- input current from mains [0.05A/div], CH2- current consumption of radio station from 12Vdc [1A/div].

The oscilloscopic records in Fig. 7 show the consumption of the radio station (the most critical consumer in the system) in all three operating modes (receiving, "stand-by" mode and transmission).

Fig. 7 (a) shows the battery voltage of 12Vdc and the current consumption of the radio station in the mentioned three modes. The recording shows that the maximum current consumption of the radio station is in the transmission mode (TRANSMIT) and in the receiving mode (RECIEVE) it is about 3.5A. The duration of the transmission time interval is about 100ms, and the duration of the receiving time interval is about 25ms. The obtained oscilloscopic records correspond to the theoretical diagram of the current consumption of the radio station given in Fig. 5. Fig. 7 (b) shows the input current from the mains (AC network 230V, 50Hz) and current consumption from 12Vdc battery.

Detailed representations of the current consumption of

the radio station supplied from 12Vdc and the current consumption of the system supplied from the power supply network (when the mains AC charger is switched on) are given in Fig. 8. Fig. 8 (a) shows recorded waveforms of input mains currents and current consumption from 12Vdc in transmission mode, while in Fig. 8 (b) are shown the same waveforms in receiving mode and in "stand-by" mode.

Fig. 9 shows the waveforms of the mains voltage and the input current of the charger for the characteristic operating modes of the system.

Fig. 9 (a) shows the recorded waveforms of the mains voltage and input mains current in the transmission mode of the radio station (the most critical case). In this mode, a relatively favorable power factor (PF>0.9) is achieved. Fig. 9 (b) shows the same waveforms, but in the signal receiving mode and in "stand-by" mode. In this case, the power factor of the system is worse (it is mostly capacitive).
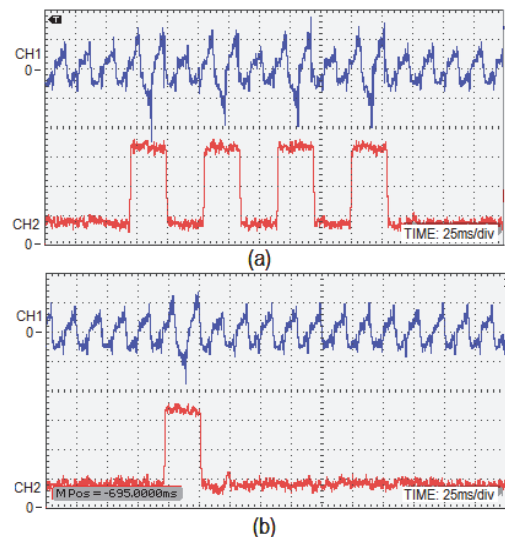

Fig. 8. Detailed oscilloscopic records of radio station consumption; (a) TRANSMITT mode; CH1-input mains current [0.05A/div], CH2- current of radio station consumption [1A/div], (b) RECIEVE mode; CH1-input mains current [0.05A/div], CH2- radio station consumption [1A/div].

Fig. 10 shows the characteristic waveforms of the battery voltage and current of the MPPT charger when it is powered from the solar panel in the time interval with the highest solar insolation (around noon).

Fig. 10 (a) shows the battery charging start mode from an initial voltage of 10.8V (fully discharged battery - battery discharge about 80%), while Fig. 10 (b) shows the completion of battery charging, i.e., the battery has reached a charge state of about 100 %. This image shows a small drop in battery voltage when the charger switches to "trickle charge" mode.

VI. REALIZATION OF HYBRID POWER SYSTEM

Within the project, a two-sided power supply was realized: mains power supply 230V, 50Hz from the street lighting pole and a solar power supply realized from a solar panel with a power of 160W. A power distribution cabinet, control, measuring and telecommunication equipment, a

solar panel, as well as the antenna of the radio station are mounted on a metal racket in the form of a compact frame. Fig. 11 shows the appearance of a prefabricated steel frame with associated equipment.
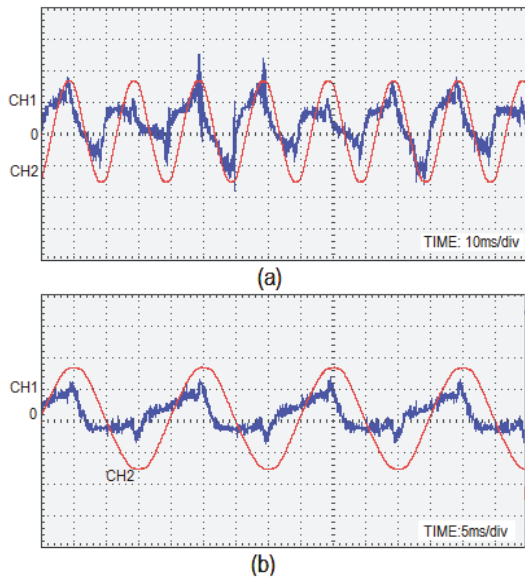

Fig. 9 Input current and voltage of mains (power network) charger; (a) TRANSMITT mode: CH1- input mains current [0.05A/div], CH2-mains voltage [200V/div], (b) STAND-BY mode (low consumption): CH1- input mains current [0.05A/div], CH2-mains voltage [200V/div].
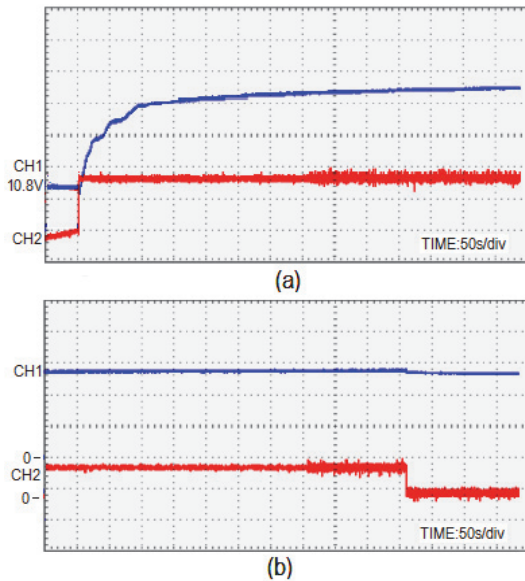

Fig. 10. Charging regime of battery from the solar panel: (a) time interval at the beginning of charging: battery voltage CH1-[500mV/div], charging current CH2-[5A/div], (b) time interval at the end of charging: battery voltage CH1-[5V/div], charging current CH2-[2A/div]

Fig. 11 (a) shows the distribution cabinet and radio station antenna. Fig. 11 (b) shows the installation details of the radio station antenna, lightning rod and solar panel. Fig. 11 (c) shows the disposition of the inner mounting plate of the hybrid power distribution cabinet and the arrangement of the associated equipment.

The following elements are placed on the mounting plate inside the distribution cabinet:
(1) PIN-3 wired level indicator electronics, (2) KIDS-16 digital input module, (3) XBB protocol converter module, (4) radio station, (5) AC grid power charger, (6) MPPT solar charger, (7) battery bank 12Vdc/2x55Ah, (8) mains terminals of mains (AC) connection 230V, 50Hz (L1, N, PE), (9) connection terminals of cable from solar panel, (10) heater and fan inside the cabinet with associated thermostat and hygrostat.
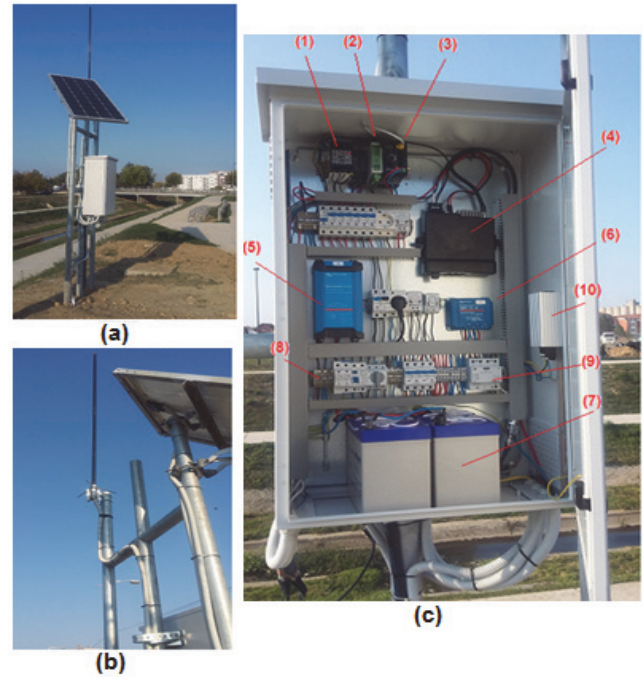

Fig. 11. Appearance of the mounting frame with associated equipment; (a) solar panel, power distribution cabinet and radio station antenna, (b) detail of PV panel and antenna installation, (c) inner mounting plate of the hybrid power distribution cabinet.

VII. Conclusion

The paper presents the key experimental and implementation results of the design of hybrid power supply system for a measuring station on the river Ub, municipality of Ub. This station is an integral part of the flood protection system. All necessary measuring and telecommunication equipment is provided within the measuring station. Based on the main project, the power supply system was realized at the end of October 2019. A two-sided power supply was performed: during the day, the dominant source is solar energy, belonging to the MPPT charger and battery bank, while during the night, the dominant source is the power AC grid 230V, 50Hz (obtained from the nearest street lighting pole). The system has been in operation since November 2019. The Emergency Management Sector of the Republic of Serbia (Command Control Center of the Municipality of Ub) is the user of the realized hybrid power supply system.

REFERENCES

[1] C.V. Nayar, M. Ashari, W.W.L. Keerthipala, "A grid-interactive photovoltaic uninterruptible power supply system using battery storage and a back-up diesel generator", *IEEE Trans. on Energy Conversion*, Vol. 15, iss. 3, pp. 348 – 353, Sep 2000.

[2] S. Rehman and I. El-Amin, "Study of a solar pv/wind/diesel hybrid power system for a remotely located population near Arar, Saudi Arabia", *ENERGY EXPLORATION & EXPLOITATION*, Vol.33, No4, 2015, pp. 591–620.

[3] M.Batic, A.Vitorovic, Z.Despotovic, "The Consideration of Optimal Control Algorithms for Hybrid Renewable Energy Systems", *XVI International Conference YU INFO 2010*, Kopaonik, 03-06.03.2010.

[4] M. M. Mahmoud and I. H. Ibrik, "Techno-economic feasibility of energy supply of remote villages in Palestine by PV-systems, diesel generators and electric grid", *Renewable and Sustainable Energy Reviews*, vol. 10, no. 2, pp. 128–138, 2006.

[5] S.S.Durgam, A.B.Musale, S.A.Balki, P.S.Gahane, L.B. Awale, "AC Hybrid Charge Controller", *Int. Journal of Engineering Research and Applications*, Vol. 5, Issue 3, (Part -5) March 2015, pp.5-10

[6] C.L.Shen, Y.X.Ko, "Hybrid-input power supply with PFC (power factor corrector) and MPPT (maximum power point tracking) features for battery charging and HB-LED driving", *Energy*, Vol.72, No.1, August 2014, pp.501-509.

[7] H.Fakham, D.Lu, B.Francois, "Power Control Design of a battery charger in a Hybrid Active PV generator for load following applications", *IEEE Transaction on Industrial Electronics*, Vol. 58, Iss. 1 , pp. 85-94, Jan. 2011, TIE-09-1370.

[8] M.A. Omar and M.M. Mahmoud, "Design and Simulation of a PV System Operating in Grid-Connected and Stand-Alone Modes for Areas of Daily Grid Blackouts", *International Journal of Photoenergy*, Volume 2019, Article ID 5216583, 9 pages, https://doi.org/10.1155/2019/5216583

[9] M. Alramlawi, A. Gabash, E. Mohagheghi, and P. Li, "Optimal operation of hybrid PV-battery system considering grid scheduled blackouts and battery lifetime", *Solar Energy*, vol. 161, pp. 125–137, 2018.

[10] M. Tajdić, Ž. V. Despotović and J. Kon, "Design and Implementation of an Uninterruptible Power Supply for Command and Control Center of the Surveillance, Alert & Warning System", *20th International Symposium INFOTEH-JAHORINA (INFOTEH), 2021*, pp.1-6; https://ieeexplore.ieee.org/document/9400686

[11] Y. K. Lo, H. J. Chiu, T. P. Lee, I. Purnama, J. M. Wang, "Analysis and Design of a Photovoltaic System DC connected to the Utility With a Power Factor Corrector", *IEEE Transaction on Industrial Electronics*, vol.56, iss. 11, pp. 4354- 4362, Nov. 2009.

[12] Ž. V. Despotović and M. Tajdić, "Design and Implementation of a Hybrid Power for Telecommunication and Measuring Remote Station of the Surveillance, Alert and Warning System", *29th Telecommunications Forum (TELFOR), 2021*, pp. 1-4, doi: 10.1109/TELFOR52709.2021.9653255.

[13] Ž.V.Despotović, I.R.Stevanović, "Hybrid Power Supply of the Agrokapilaris® System for Irrigation of Vegatable Crops on the Plot Grabovac –Obrenovac", *International symposium POWER PLANTS 2021*, Belgrade 17-18 November, Serbia.

[14] G. Delille, B. François, "A review of some technical and economic features of energy storage technologies for distribution system integration", *Ecological engineering and environment protection*, pp. 40-48, vol. 1, ISSN 1311 – 8668, 2009.

[15] A.A.A.Alahmadi et al., "Hybrid Wind/PV/Battery Energy Management-Based Intelligent Non-Integer Control for Smart DC-Microgrid of Smart University", *IEEE Access*, vol. 9, pp. 98948-98961, 2021, doi: 10.1109/ACCESS.2021.3095973.

[16] B. Đorđević and Ž. V. Despotović, "Digital Control of Four Switch Synchronous Buck-Boost Power Converter based on PIC18F4520 Microcontroller", *20th International Symposium INFOTEH-JAHORINA (INFOTEH)*, 2021, pp. 1-6, doi: 10.1109/INFOTEH51037.2021.9400656.